

Fah-KO(M-NSG)

敲除Fah基因exon 3，建立Fah基因敲除小鼠模型。

品系全名	NOD.Cg-Prkdc ^{scid} Il2rg ^{em1} Fah ^{em2Smoc}
目录号	NM-NSG-004
品系状态	精子冻存

基因信息

基因名 Fah	基因曾用名	swst
	NCBI ID	14085
	MGI ID	95482
	Ensembl ID	ENSMUSG00000030630
	人类同源基因	FAH

品系描述

敲除Fah基因exon 3，建立Fah基因敲除小鼠模型。

应用领域： 酪胺酸血症第一型研究相关

*使用本品系发表的文献需注明: Fah-KO(M-NSG) mice (Cat. NO. NM-NSG-004) were purchased from Shanghai Model Organisms Center, Inc..

验证数据

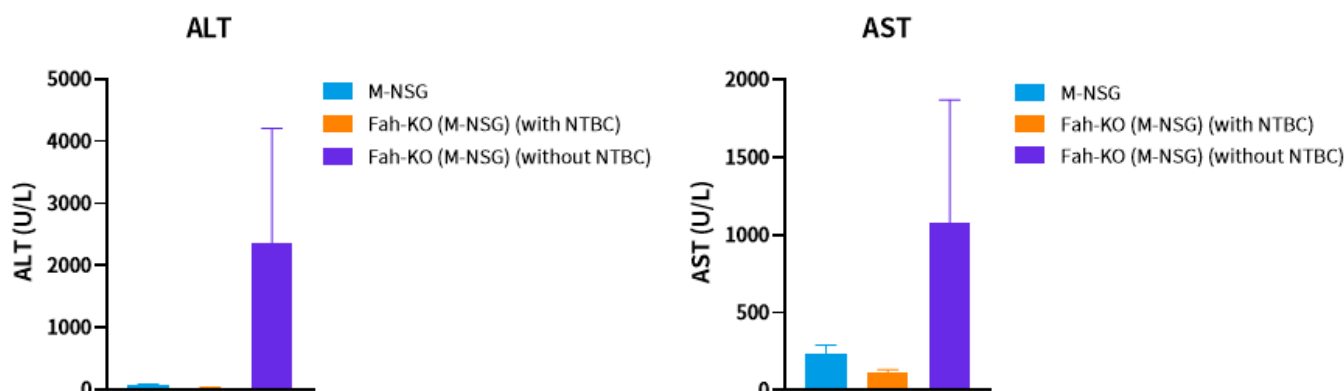


Fig.1 Detection of liver function by blood biochemistry.

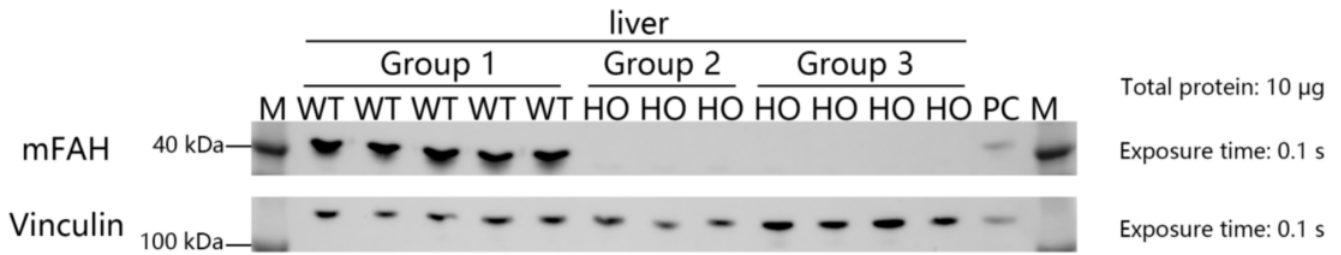


Fig.2 Detection of FAH expression in Fah-KO(M-NSG) mice by WB. 14-week-old male mice were utilized in this study. On Day 0, NTBC (2-(2-nitro-4-trifluoromethylbenzoyl)-1,3-cyclohexanedione) was withdrawn from the Fah-KO (M-NSG) mice in Group 3 and replaced with distilled water (ddH₂O), consistent with M-NSG mice in Group 1. Conversely, the Fah-KO (M-NSG) mice in Group 2 received continuous treatment with water containing NTBC (16 mg/L). The liver tissue lysates were collected on Day 14, and then analyzed by western blot.

Abbr. HO, homozygous; WT, wild type; PC, positive control, HepG2 cells.

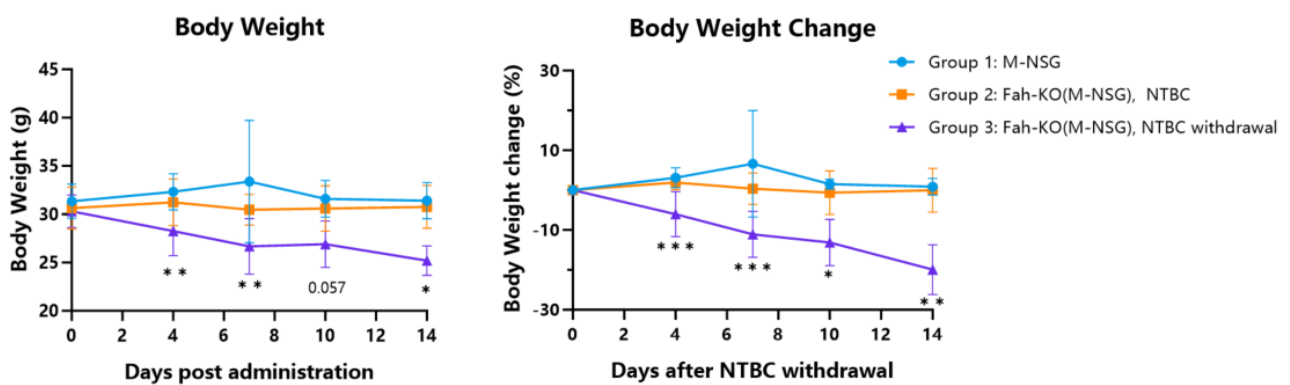


Fig.3 Body weight change of Fah-KO(M-NSG) mice following NTBC withdrawal. Following NTBC withdrawal, Fah-KO(M-NSG) mice exhibited a significant reduction of body weight. 14-week-old male mice were utilized in this study. On Day 0, NTBC was withdrawn from the Fah-KO (M-NSG) mice in Group 3 and replaced with ddH₂O, consistent with the M-NSG mice in Group 1. Conversely, the Fah-KO (M-NSG) mice in Group 2 received continuous treatment with water containing NTBC (16 mg/L). The body weight was recorded following NTBC withdrawal. (n=3-18, Mean ± SEM, t-test, Group 2 versus Group 3, **p*<0.05, ***p*<0.01, ****p*<0.001).

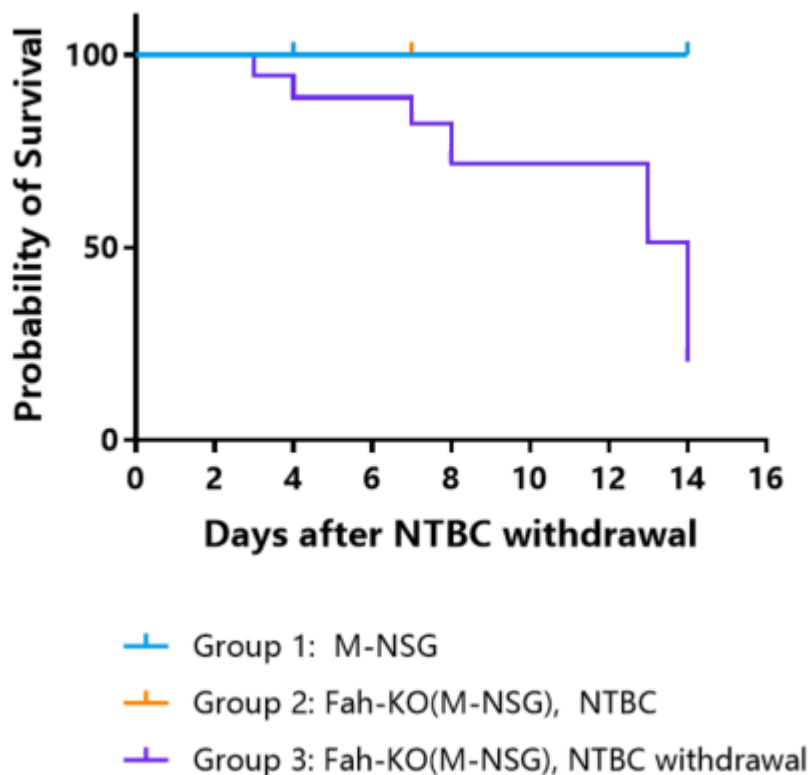


Fig.4 Survival curve of Fah-KO (M-NSG) mice following NTBC withdrawal. Following NTBC withdrawal, Fah-KO(M-NSG) mice died off due to the loss of fumarylacetoacetate hydrolase function. 14-week-old male mice were utilized in this study. On Day 0, NTBC was withdrawn from the Fah-KO (M-NSG) mice in Group 3 and replaced with ddH₂O, consistent with the M-NSG mice in Group 1. Conversely, the Fah-KO (M-NSG) mice in Group 2 received continuous treatment with water containing NTBC (16 mg/L). The survival curve was recorded following NTBC withdrawal. Three mice in each group were sacrificed on Day 4, and 3-4 mice in Groups 2 and 3 were sacrificed on Day 7. At the experimental endpoint (Day 14), two mice in Group 3 exhibited a >20% reduction in body weight; consequently, these two mice were recorded as mortality events.

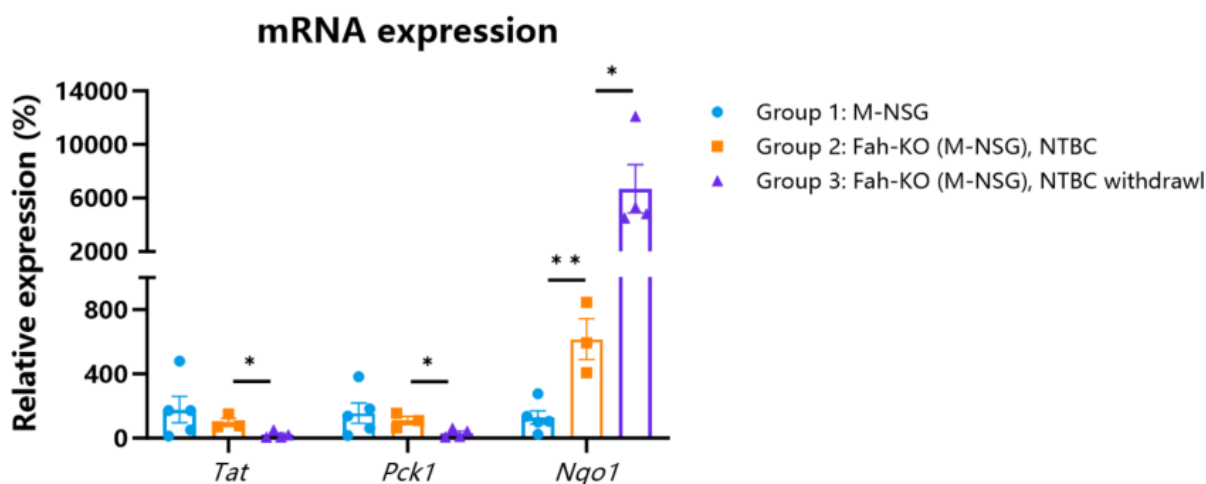


Fig.5 Detection of *Tat*, *Pcsk1* and *Nqo-1* expression in the liver of Fah-KO (M-NSG) mice by

qPCR. Consistent with previous reports, the mRNA expression of cAMP-inducible genes *Tat* and *Pcsk1* in liver tissues was significantly reduced in Fah-KO (M-NSG) mice after NTBC withdrawal. Meanwhile, the mRNA expression of the gene for oxidative damage *Nqo1* robustly increased in Fah-KO (M-NSG) mice after NTBC withdrawal. 14-week-old male mice were utilized in this study. On Day 0, NTBC was withdrawn from the Fah-KO (M-NSG) mice in Group 3 and replaced with ddH₂O, consistent with the M-NSG mice in Group 1. Conversely, the Fah-KO (M-NSG) mice in Group 2 received continuous treatment with water containing NTBC (16 mg/L). Liver tissues were collected on Day 14 and were performed RNA extraction. Then cDNA libraries were synthesized by reverse transcription, followed by qPCR with mouse *Tat*, *Pck1*, *Nqo1* and *Gapdh* primers. Relative expression represents the mouse *Tat*, *Pck1* and *Nqo1* mRNA level relative to its average expression in Group 1.

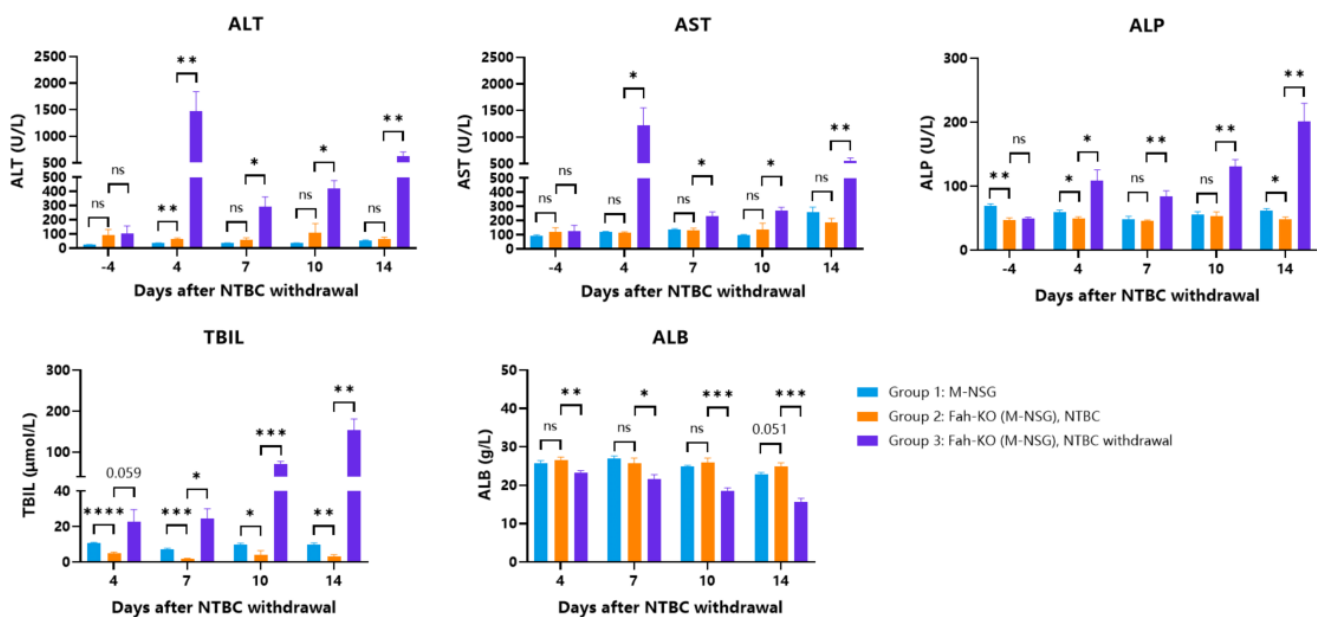


Fig.6 Biochemical assessment of hepatic function of Fah-KO(M-NSG) mice following NTBC withdrawal. Following NTBC withdrawal, Fah-KO(M-NSG) mice exhibited a significant elevation in serum ALT, AST, ALP and TBIL levels, accompanied by a marked reduction in ALB levels. These alterations are indicative of acute and severe hepatic impairment resulting from the loss of fumarylacetoacetate hydrolase function. 14-week-old male mice were utilized in this study. On Day 0, NTBC was withdrawn from the Fah-KO (M-NSG) mice in Group 3 and replaced with ddH₂O, consistent with the M-NSG mice in Group 1. Conversely, the Fah-KO (M-NSG) mice in Group 2 received continuous treatment with water containing NTBC (16 mg/L). Serum samples were collected at specified intervals to quantify the levels of (A) alanine transaminase (ALT), (B) aspartate aminotransferase (AST), (C) alkaline phosphatase (ALP), (D) total bilirubin (TBIL), and (E) albumin (ALB). (n=3-18, Mean ± SEM, t-test, * $p < 0.05$, ** $p < 0.01$, *** $p < 0.001$, **** $p < 0.0001$, ns, no significance).

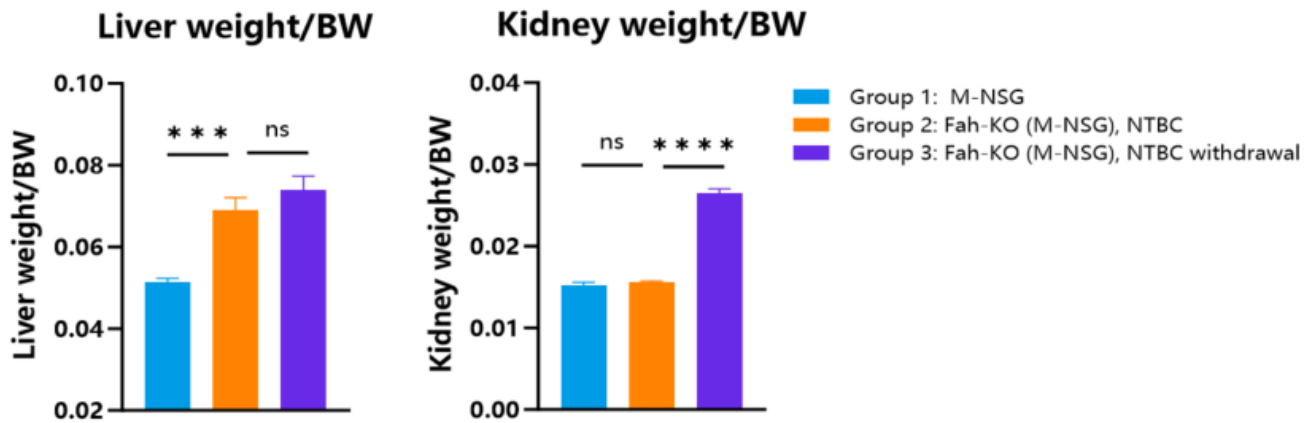


Fig.7 Liver and kidney weights of Fah-KO (M-NSG) mice following NTBC withdrawal. The relative liver weight of Fah-KO (M-NSG) mice was significantly higher than that of N-NSG controls. Following NTBC withdrawal, a marked increase in relative kidney weight was also observed in the Fah-KO group. These elevations in relative organ weights are indicative of severe hepatic and renal injury induced by the loss of Fah and subsequent NTBC cessation. 14-week-old male mice were utilized in this study. On Day 0, NTBC was withdrawn from the Fah-KO (M-NSG) mice in Group 3 and replaced with ddH₂O, consistent with the M-NSG mice in Group 1. Conversely, the Fah-KO (M-NSG) mice in Group 2 received continuous treatment with water containing NTBC (16 mg/L). Liver and kidney weights were recorded on Day 14 (n=3-5, Mean±SEM, Unpaired t-test, *** p <0.001, **** p <0.0001, ns: no significance).

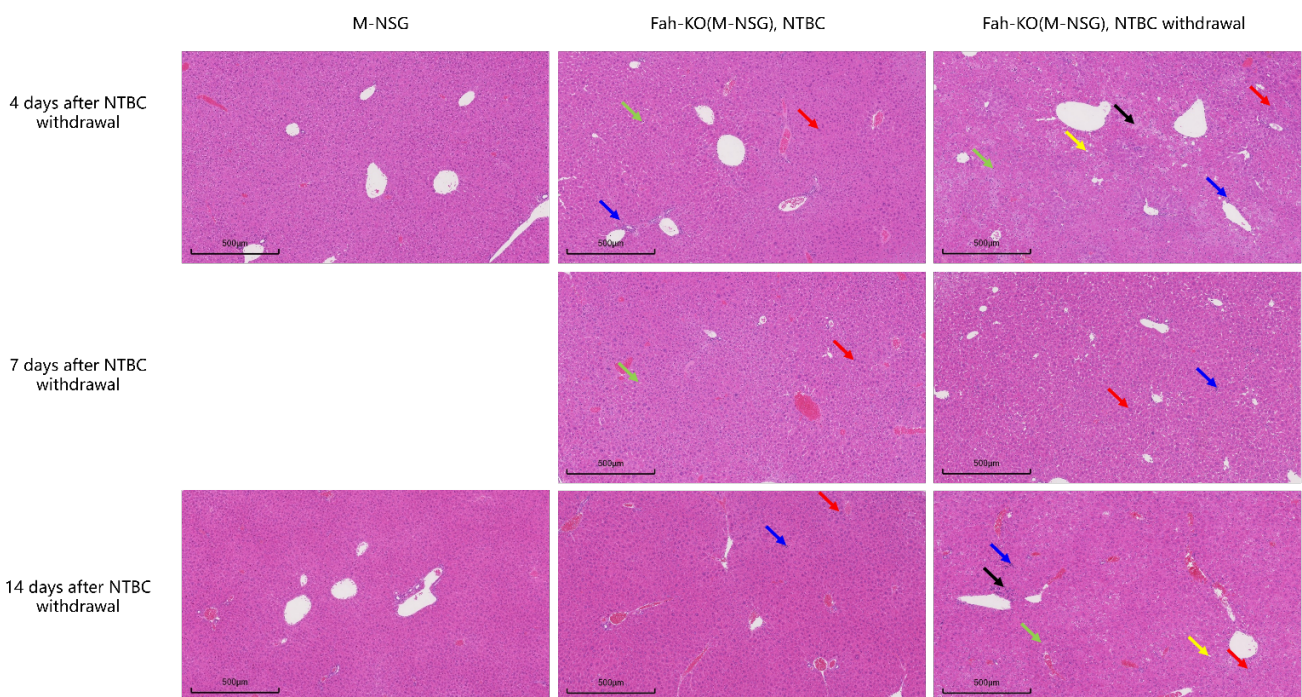


Fig.8 Representative histopathological images of liver following NTBC withdrawal (n=3-5, male). Pathological features include hepatocyte steatosis (yellow arrow), inflammatory cell infiltration (blue arrow), hepatocyte hypertrophy (red arrow), necrosis (black arrow) and Kupffer cell activation (green arrow).

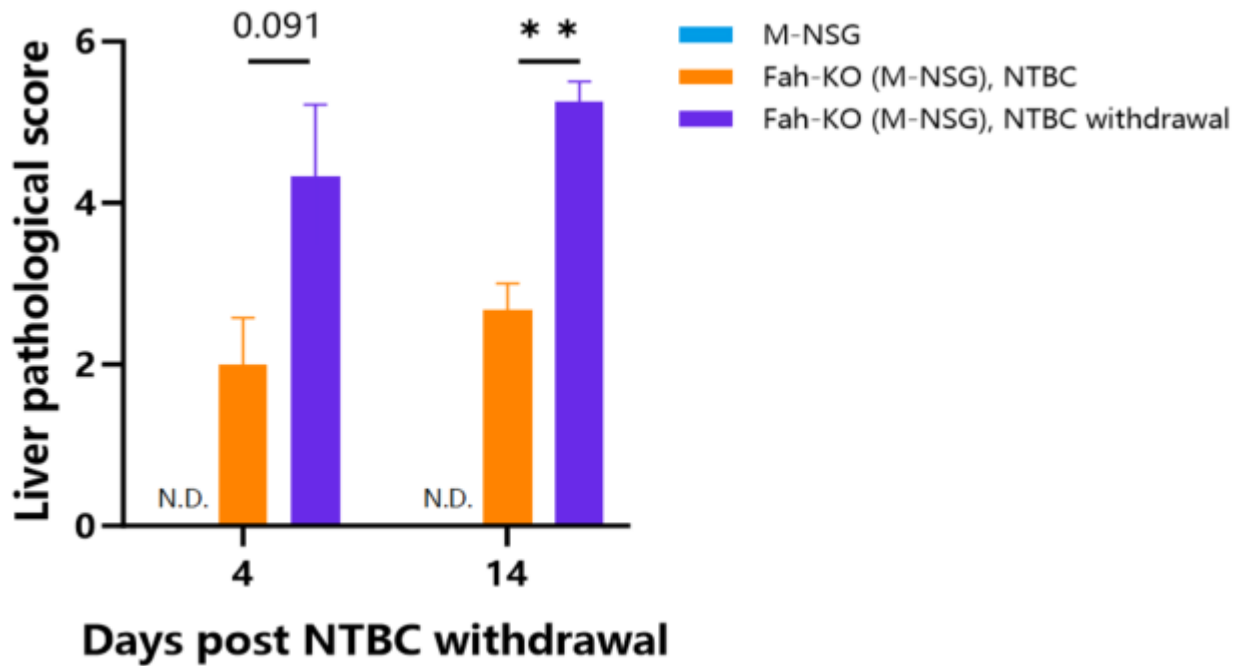


Fig.9 Liver pathological scores of male Fah-KO (M-NSG) mice at days 4, 7, and 14 post-NTBC withdrawal. Following NTBC withdrawal, Fah-KO (M-NSG) mice developed significant hepatic injury, characterized by moderate fatty degeneration, inflammatory cell infiltration, hepatocyte hypertrophy, necrosis, and mild activation of Kupffer cells. (n=3-5, Mean±SEM, Unpaired t-test, ** $p < 0.01$, ns: no significance).

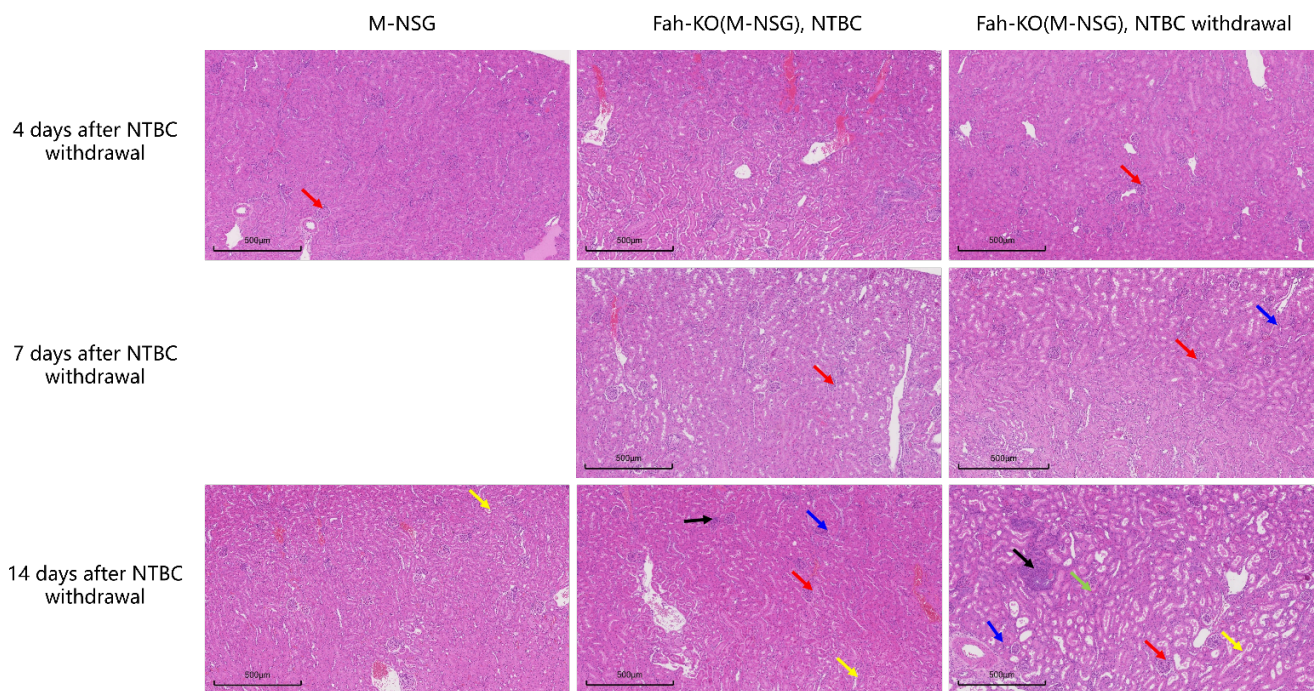


Fig.10 Representative histopathological images of kidney after NTBC withdrawal (n=3-5, male). Pathological features include tubular degeneration and atrophy (yellow arrows), increased basophilia (green arrows), necrosis (black arrows), mesangial proliferation of glomeruli (red arrows), fibrosis (white arrows), and inflammatory cell infiltration (blue arrows).

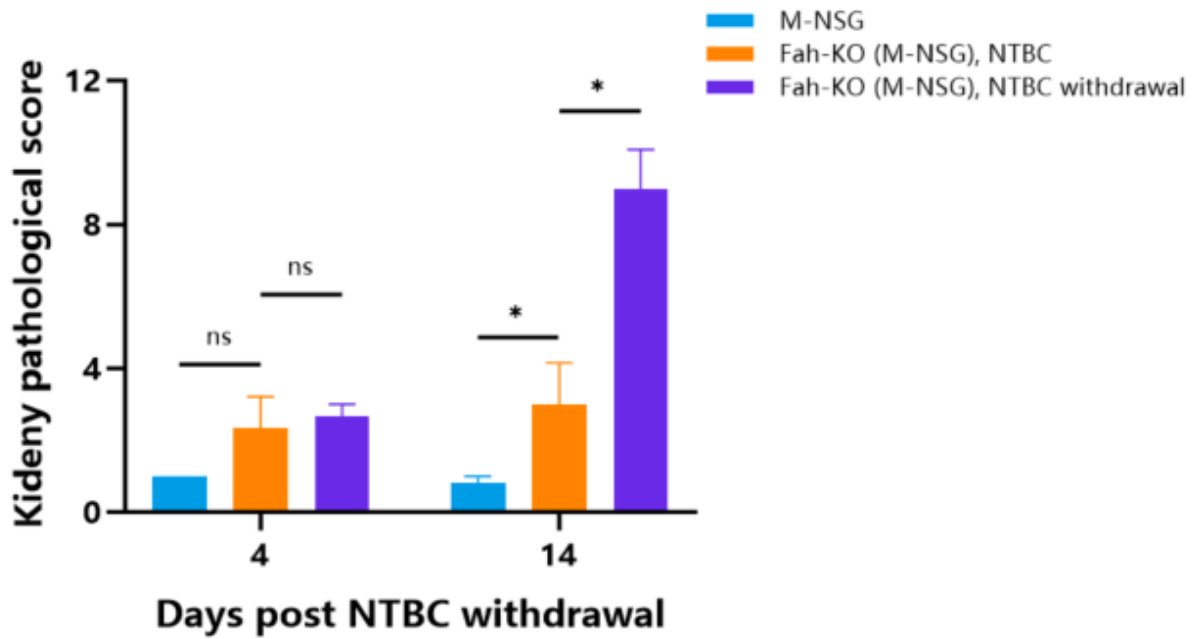


Fig.11 Kidney pathological scores of male Fah-KO (M-NSG) mice at days 4, 7, and 14 post-NTBC withdrawal. (n=3-5, Mean±SEM, Unpaired t-test, * $p < 0.05$, ns: no significance). Following NTBC withdrawal, Fah-KO (M-NSG) mice exhibited significant renal injury characterized by moderate tubular degeneration and atrophy, epithelial cells desquamation and necrosis and increased basophilia. Furthermore, histopathological examination revealed mesangial thickening within the glomeruli, along with inflammatory cell infiltration in the renal interstitium and sporadic interstitial fibrosis.